The repair and regeneration mechanism of platelet-rich fibrin-promoting tissue after alveolar bone defect through the notch pathway

Tao Li, Hui Long, Wei Niu, Bo Feng*

Department of Prosthodontics, Changsha Stomatological Hospital, Hunan University of Chinese Medicine, Changsha 410004, Hunan Province, China

ARTICLE INFO

ABSTRACT

This work investigated the effects of platelet-rich fibrin (PRF) combined with bone mesenchymal stem cells (BMSCs) on the repair of alveolar bone defect (ABD) and the related mechanism of the Notch1/Wnt3a signaling pathway. 28 healthy male New Zealand white rabbits were selected to prepare the BMSCs and PRF. Rabbits were rolled into a combination group (implanted with PRF + BMSCs for treatment), a PRF group (treated with PRF) a BMSC group (BMSCs for treatment), and a control group (Ctrl group, no material implantation), with 7 rabbits in each. The Notch1, Wnt3a, bone morphogenetic protein 9 (BMP9), and p-JNK in rabbits in various groups were compared. It was found that Notch1 and Wnt3a in the combination group were sharply higher than those in the PRF and BMSC groups at postoperative 5 and 10 weeks, exhibiting great differences ($P<0.05$). The osteocalcin (OCN) and alkaline phosphatase (ALP) in the combination group were higher based on those in the PRF group, BMSC group, and Ctrl group (all $P<0.05$). Meanwhile, BMP9 and P-JNK proteins in the combination group were much higher than those in the PRF, BMSC, and Ctrl groups, presenting obvious differences ($P<0.05$). The results revealed that PRF + BMSCs could more effectively downregulate the Notch1 and Wnt3a and activate the Notch1/Wnt3a signaling pathway, thus promoting the osteogenesis of ABD and improving the repair effect.

Introduction

The alveolar bone is part of the jaw that surrounds the root of the tooth and is closely connected to the root by the periodontal membrane. The bone pit where the root of the tooth is located is called the alveolar fossa (1). Both alveolar bone and periodontal membrane play a role in supporting and fixing teeth, while alveolar bone defect (ABD) refers to the tissue defect in this part, which seriously affects the oral health of patients (2,3). The causes of ABD are very complex. For example, if the teeth are not filled in time after falling out, the alveolar bone will be slowly absorbed, resulting in symptoms of ABD (4). There are also many patients due to apical inflammation, root inflammation and others not received timely treatment, resulting in inflammation to stimulate the alveolar bone, and eventually leading to ABD. In addition, there is trauma, such as traffic accidents, sports injuries, fighting, etc., which may cause self-fracture and defect of alveolar bone due to external forces (5,6). Treatments vary depending on what causes ABD. If ABD is caused by tooth loss, in order to avoid this consequence, you can timely fill the teeth, with dentures, dentures, etc., to replace your teeth. If ABD is caused by trauma, the alveolar bone can be repaired by surgery (7). For those patients with ABD caused by dental diseases, it is necessary to conduct treatment on the first tooth to clean out the necrotic tissue inside the tooth and involve the root canal of the leaf. Timely root canal treatment is also required before the alveolar bone can be repaired (8,9).

Guided tissue regeneration (GTR) is a new technique developed on the basis of the understanding of the potential of periodontal tissue regeneration in the 1970s. It makes the therapeutic effect of periodontitis reach a higher level and can regenerate the periodontal tissues destroyed by periodontitis, including cementum, periodontal membrane and alveolar bone, and form new attachments (10). The basic principle of GTR is to prevent root migration of the epithelium (preventing connective tissue from contacting the root surface) and provide space by placing a membrane between the flap and the root surface of the tooth. Cells derived from the periodontal membrane are selectively guided to the root surface to form new adhesion healing, so as to achieve the purpose of periodontal tissue regeneration (11-13). Platelet-rich fibrin (PRF), a concentration of white blood cells and PRF matrix, has a molecular structure similar to natural blood clots and enables tissue repair through the regulatory effects of cytokines and the role of fibrin as a scaffold. Mesenchymal stem cells (MSCs), another important member of the stem cell family, originate from the mesoderm and ectoderm in early development (14). MSCs are adult stem cells with self-replication ability and multidirectional differentiation potential, belonging to non-terminal differentiated cells, which have the characteristics of both mesenchymal cells, endothelial and epithelial cells (15). Under specific induction conditions in vitro, MSCs can differentiate into adipose, cartilage, bone, muscle, tendon, nerve, liver, myocardial, islet beta cells,

* Corresponding author. Email: qibeixi83494443656@163.com

endothelial cells and other tissue cells, which still have the potential of multidirection differentiation after continuous subculture and cryo-preservation (16,17). Bone MSCs (BMSCs) are a kind of adult stem cells originating from mesoderm, with self-renewal and multi-differentiation potential, and can differentiate into various interstitial tissues, such as bone, cartilage, fat, bone marrow hematopoietic tissues, etc. (18).

In summary, the application effect and mechanism of PRF in ABD repair remain unclear. In this work, 28 healthy male New Zealand white rabbits purchased from the Animal Center of the University were selected to prepare the BMSCs and PRFS. According to different treatment methods, all white rabbits were rolled into a combination group (PRF + BMSCs), a PRF group, a BMSC group (BMSCs), and a Ctrl group (no material implantation), with 7 rabbits in each. The expressions of Notch1, Wnt3a, BMP9, and p-JNK proteins in rabbits in various groups were compared to further explore the effects of PRF combined with BMSCs on ABD repair and the mechanism related to the Notch1/Wnt3a signaling pathway.

Materials and Methods

Experimental animals

Twenty-eight healthy male New Zealand white rabbits, weighing 3 ± 0.5 kg, were selected from the Animal Center of the University. They were adaptively fed for 1 week, the relative humidity was maintained at about 50%, indoor temperature was maintained at 23 - 25℃, they free diet and water, and then continuously fed for 5 weeks.

Preparation of BMSCs

After the rabbits were disinfected, the medical sterilization bone marrow puncture needle was inserted into the rabbit bone marrow cavity, and 4 mL of rabbit bone marrow was extracted. The cells were isolated by cell density separation and cultured in Dulbeco Modified Eagle Medium (DMEM) at 37℃ and 5%CO_2. The liquid was updated after 48 hours and then every 3 days. The cells were digested with 0.25% pancreatic enzymes when the growth reached 90% and centrifuged at 1,500 rpm for 5 min. The third-generation BMSCs were obtained by subculture at the ratio of 1:2.

Preparation of PRF

10 mL of rabbit ear border arterial blood was extracted and centrifuged at 3,500 rpm for 20 min. The centrifuge tube was leveled into 3 layers, namely the red blood cell layer, white gel layer, and serum layer. PRF gel was obtained from the middle layer and cultured at 37℃ and 5%CO_2 so that 1.2×10^6 cells existed on each PRF gel.

Construction and grouping of rat models

According to different treatment methods, all white rabbits were rolled into a combination group, a PRF group, a BMSC group, and a Ctrl group, with n = 7 all. The rabbits were implanted with PRF + BMSCs in the combination group, PRF in the PRF group, BMSCs in the BMSC group, and without any material in the Ctrl group. All the rabbits in the four groups were closely sutured gingival and periodontal dressing covered the wound.

Treatment of alveolar bone specimens

At 3, 6, and 9 weeks after surgery, samples were taken from the anterior mandibular area of rats, and the bone fragments were fixed in 4% paraformaldehyde for 2 days. The specimen was decalcified by placing it in 40% formic acid and changing it daily until the needle no longer felt resistance when inserted. The samples were then put into 5% potassium sulfate for 12 hours, and washed with water 2 days later. The samples were dehydrated by gradient ethanol, hyaline by toluene, and infiltrated by paraffin. Finally, the specimens were embedded parallel to the long tooth axis in the embedding direction and sliced.

HE staining

The paraffin sections were placed in the oven for 1 hour, immersed in toluene for 30 minutes, hydrated with gradient ethanol and stained with hematoxylin solution for 10 minutes, and rinsed with running water for 5 minutes. Then, the specimen was placed into 1% saline ethanol for hydration for half a minute, rinsed with water for 3 minutes, added with 0.2% ammonia water reaction for 1 minute, and then rinsed with tap water for 5 minutes. The slices were put into an eosin staining solution for 3 minutes, and the cytoplasm was stained. The slices were dehydrated with gradient ethanol, treated with xylene transparent, sealed with neutral gum, and observed with a high-definition microscope after drying.

Immunohistochemical staining

After dewaxing and hydration, the paraffin sections were irradiated with a microwave for 15 minutes, and the sections were thawed until room temperature. The slices were then placed into sodium citrate buffer at pH 6.5 and cleaned 3 times with phosphate buffer for 5 minutes each time. After the sheep serum was sealed, the samples were incubated at 37℃ for 30 minutes. A primary antibody was added to the pretreated sections. A large suction head was first used to add antibody diluent, a small suction head was changed to add antibody, and then a large suction head was used to mix. Then the secondary antibody was added and the reaction was carried out at 37℃ for 30 min. The phosphate buffer was cleaned 3 times for 5 min each time. Diaminobenzidine (DAB) color development solution was added to illustrate, color development time was controlled under the microscope, and color development was terminated by distilled water. The sample was restained with hematoxylin for 3 minutes and rinsed with water 3 times. Furthermore, 1% hydrochloric acid ethanol was added for differentiation for 25 seconds, rinsed with water twice, then put in PBS for blue return for 5 minutes, and placed in gradient alcohol to soak and dehydrate for xylene transparent for 20 seconds. Next, the neutral gum was employed for the seal, and then it was observed under an HD microscope.

Observed indicators

1. The healing effect of soft and hard tissue, alveolar bone fullness and bone absorption were observed before surgery, 5 weeks, and 10 weeks after tooth extraction.
2. HE-stained sections were observed under an HD microscope to record the formation and degradation of new bone in tooth extraction fossa.
3. Immunohistochemical observation was performed as follows: 10 high-power visual fields of rabbit bone defects

were selected from each group, and the average optical density (AOD) of Notch1 and Wnt3a in each group was measured by Image-Pro Plus.

4. The expression levels of osteocalcin (OCN) and alkaline phosphatase (ALP) in the serum of rabbits in the four groups were determined by enzyme-related immunosorbent assay.

5. The protein expression levels of BMP9, c-JNK, and p-JNK in new bone tissue of rabbits in the four groups were determined by western blotting.

Methods for statistics

The research data processing adopted SPSS19.0, measurement data were expressed with mean ± standard deviation ($\bar{x} \pm s$), and count data were expressed as percentage (%). Repeated measure analysis of variance was used for inter-group comparison, and two-factor analysis of variance was used for intra-group comparison. By bilateral test, $P<0.05$ suggested a statistically significant difference.

Results

Gross and HE staining of rabbits in two groups were observed

All the rabbits survived well, the color of oral gingival mucosa was normal, and the extraction wound healed well without infection and suppuration.

At 5 weeks after the operation, the labial bone plates of the combination group of rabbits were full, and bone cells and bone trabeculae could be seen under the microscope. PRF group rabbit alveolar bone is general, bone trabecular arrangement was disordered. The alveolar bone structure of BMSC group rabbits was poor, and the bone structure and Haversian system could be seen under the microscope. In the Ctrl group, the rabbit labial bone plate structure was complete, bone trabeculae were arranged neatly, and the tooth extraction fossa was fibrous tissue.

At 10 weeks after surgery, the labial bone plates in the combination group of rabbits were hard, new bone and bone trabeculae could be observed by the microscope, and the defect area was full of new braided bone and lamellar bone. In the PRF group, the rabbit bone trabecular system was sparse, and the number of new braided bone and lamellar bone was large. The bone trabecular system of BMSC group rabbits was sparse, the number of new braided bone and lamellar bone was more, and the number of Haversian systems was less. The labial bone wall in the Ctrl group rabbits was significantly dented, with a small amount of bone-like tissue surrounded by fibrous connective tissue.

Expression of Notch1

As illustrated in Figure 1, the Notch1 was 0.261 ± 0.075 and 0.134 ± 0.048 in the combination group, that was 0.174 ± 0.056 and 0.088 ± 0.013 in the PRF group, was 0.171 ± 0.032 and 0.079 ± 0.022 in the BMSC group, and was 0.048 ± 0.007 and 0.148 ± 0.068 in the Ctrl group after they were treated 5 and 10 weeks. Therefore, it can be concluded that the combination group presented an obviously high Notch1 level than the PRF and BMSC groups at posttreatment 5 and 10 weeks, showing great differences ($P<0.05$), but showed no great difference with that in the Ctrl group after the rabbits were treated 10 weeks ($P>0.05$).

Wnt3a

As demonstrated in Figure 2 and Figure 3, the Wnt3a was 0.228 ± 0.047 and 0.105 ± 0.032 in the combination group, that was 0.156 ± 0.034 and 0.079 ± 0.014 in the PRF group, 0.151 ± 0.028 and 0.071 ± 0.016 in the BMSC group, and was 0.049 ± 0.008 and 0.125 ± 0.051 in the Ctrl group after they were treated 5 and 10 weeks. Therefore, it can be concluded that the combination group presented an obviously high Wnt3a level than the PRF and BMSC groups at posttreatment 5 and 10 weeks, showing great differences ($P<0.05$), but showed no great difference with that in the Ctrl group after the rabbits were treated 10 weeks ($P>0.05$).

Serum OCN and ALP of rabbits in various groups

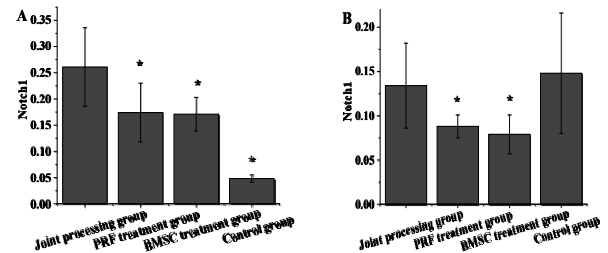Figure 4 and Figure 5 were drawn to display the OCN

Figure 1. Notch1 in rabbits in various groups (A: posttreatment 5 weeks; B: posttreatment 10 weeks). Note: * meant a great difference with $P<0.05$ to the combination group.
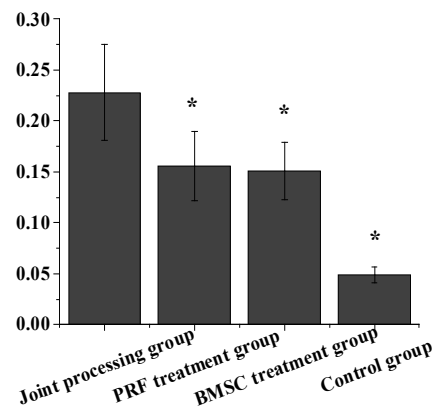

Figure 2. Wnt3a in rabbits in various groups at posttreatment 5 weeks. Note: * meant a great difference with $P<0.05$ to the combination group.
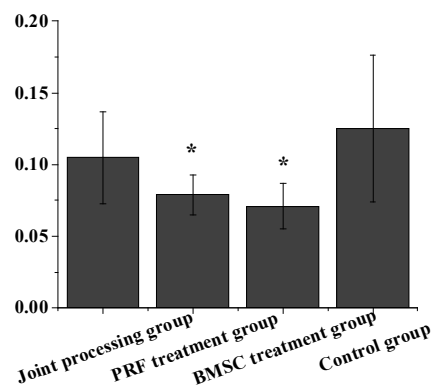

Figure 3. Wnt3a in rabbits in various groups at posttreatment 10 weeks. Note: * meant a great difference with $P<0.05$ to the combination group.

Figure 4. OCN in rabbits in various groups after they were treated with different materials. Note: * meant a great difference with $P<0.05$ to the combination group.

Figure 5. ALP in rabbits in various groups after they were treated with different materials. Note: * meant a great difference with $P<0.05$ to the combination group.
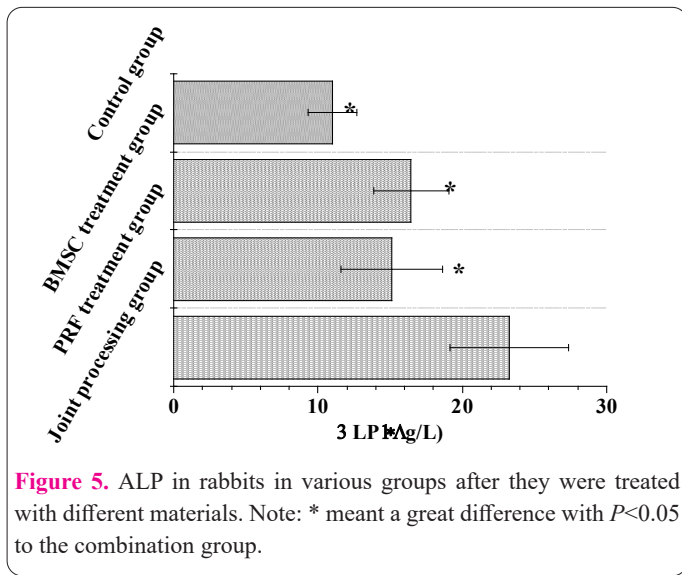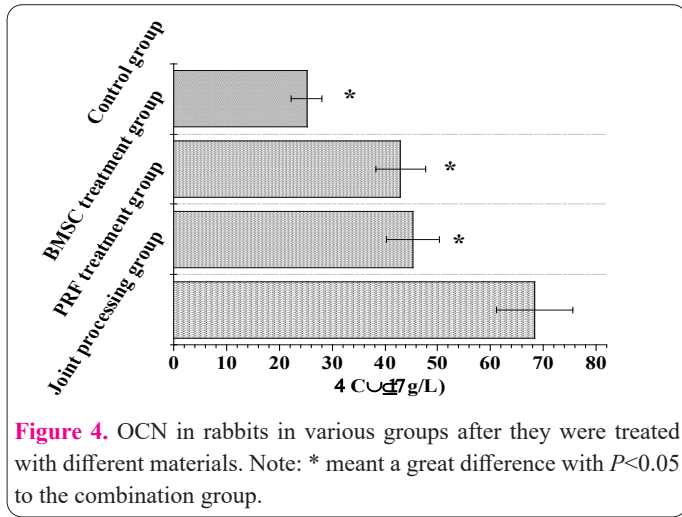
and ALP in rabbits after they were treated with different materials. The OCN and ALP in the combination group were 68.41 ± 7.22 µg/L and 23.29 ± 4.11 µg/L, respectively; those in the PRF group were 45.33 ± 5.05 µg/L and 15.08 ± 3.52 µg/L, respectively; those in the BMSC group were 42.96 ± 4.77 µg/L and 16.43 ± 2.61 µg/L, respectively; and those in the Ctrl group were 25.16 ± 2.85 µg/L and 11.02 ± 1.68 µg/L, respectively. These data suggested that the rabbits treated with PRF + BMSCs possessed obviously higher OCN and ALP levels than those treated with other materials, showing great differences ($P<0.05$).
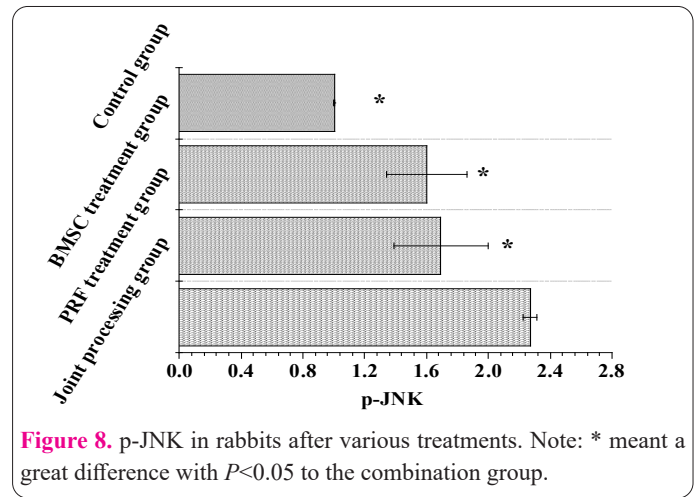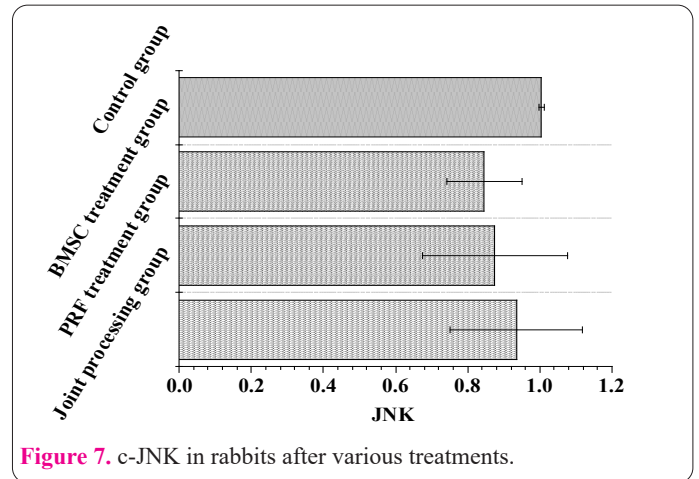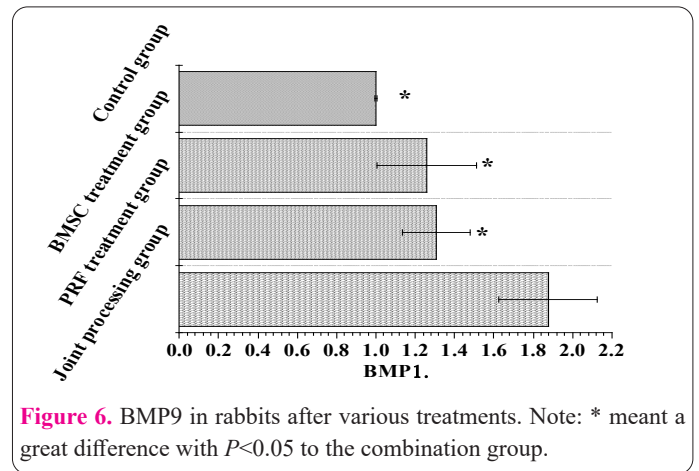
BMP9, c-JNK, and p-JNK in rabbits after they were treated with different materials

Figures 6-8 demonstrated the BMP9, c-JNK, and p-JNK in rabbits after they were treated with various materials, respectively. As the figures showed, the above three indicators in the combination groups were 1.877 ± 0.251, 0.935 ± 0.183, and 2.271 ± 0.246, respectively; those in the PRF group were 1.307 ± 0.171, 0.875 ± 0.201, and 1.692 ± 0.304, respectively; those in the BMSC group were 1.258 ± 0.255, 0.846 ± 0.105, 1.603 ± 0.259, respectively; and those in the Ctrl group were 1.000 ± 0.003, 1.005 ± 0.007, and 1.002 ± 0.005, respectively. It revealed that the BMP9 and p-JNK in rabbits treated with PRF + BMSCs were remarkably higher than the PRF, BMSC, and Ctrl group, showing obvious differences ($P<0.05$). In addition, the rabbits receiving PRF + BMSCs for treatment showed

no statistically different c-JNK level to those treated with other materials ($P>0.05$).

Discussion

ABD refers to the incompleteness of alveolar bone structure, including the discontinuity of bone structure in the three-dimensional direction, mainly manifested by bone fenestration and bone cracking. ABD may cause pathological changes in periodontal tissues and affect the tooth movement pattern and biomechanical mechanism, so it is very important for the repair and treatment of ABD (19). As a new generation of autologous blood extract, PRF is a new biomedical material rich in platelets, white blood cells and cell growth factors, and has been widely used in cell proliferation, fat transplantation, and bone tissue repair (20,21). In this work, 28 healthy male

Figure 6. BMP9 in rabbits after various treatments. Note: * meant a great difference with $P<0.05$ to the combination group.

Figure 7. c-JNK in rabbits after various treatments.

Figure 8. p-JNK in rabbits after various treatments. Note: * meant a great difference with $P<0.05$ to the combination group.

New Zealand white rabbits purchased from the Animal Center of the University were selected to prepare BMSCs and PRFS. According to different treatment methods, all white rabbits were divided into a combination group, a PRF group, a BMSC group, and a Ctrl group, with 7 rabbits in each. Firstly, Notch1 in rabbits in the combination group was higher based on that in the PRF group and the BMSC group at 5 and 10 weeks after surgery ($P<0.05$). The notch signaling pathway is a conservative and important signal transduction pathway that affects cell fate. It is involved in almost all cell proliferation and differentiation activities and plays an important role in regulating cell differentiation, proliferation, and apoptosis, as well as a series of physiological and pathological processes. These results indicate that Notch1 signals play a role in ABD repair, and PRF + BMSCs composites can more effectively promote the activation of the Notch1 signaling pathway (22). As a member of the Wnt signaling pathway family, Wnt3a signaling protein is a cysteine-rich secreted glucoprotein that binds to receptors on adjacent cell membranes through paracrine or autocrine action to activate signals at all levels in cells, regulates the related genes and the proliferation and differentiation of target cells (23). It was found that Wnt3a in rabbits in the combination group was greatly higher based on that in the PRF group and BMSC group at 5 and 10 weeks after surgery, showing statistically great differences ($P<0.05$), suggesting that the Wnt signaling pathway played a regulatory role in ABD repair.

OCN is synthesized and secreted by osteoblasts, which is relatively stable and not affected by bone resorption factors. Serum OCN can be used to understand the activity state of osteoblasts, especially newly formed osteoblasts (24). ALP is an exoenzyme of osteoblasts, and its expression activity is an obvious feature of osteoblast differentiation. The main physiological function of ALP in the body is to hydrolyze phosphate ester in the process of osteogenesis to provide necessary phosphoric acid for the deposition of hydroxyapatite, and to hydrolyze pyrophosphate to relieve its inhibition on the formation of bone salts, which is conducive to osteogenesis (25). In this work, OCN and ALP in the combination group rabbits were obviously higher when compared to those in the PRF group, BMSC group, and Ctrl group, exhibiting statistically obvious differences with $P<0.05$. This keeps in line with the results of Nguyen et al. (26), indicating that PRF + BMSCs complex can more effectively promote the formation of alveolar bone rabbit osteoblasts. Bone morphogenetic proteins, also known as bone morphogenetic proteins, are a group of highly conserved functional proteins with similar structures that can stimulate DNA synthesis and cell replication, thus promoting the directed differentiation of mesenchymal cells into osteoblasts (27). JNK family is one of the mitogen-activated protein kinases superfamily members, molecular weight 46 and 54KD stress protein kinases. The activated JNK signaling pathway plays a crucial role in regulating physiological and pathological processes such as cell differentiation, apoptosis, inflammation, stress response, ischemia-reperfusion injury, fibrosis, tumor, toxic reaction, and hyperoxia injury in clinical practice (28). This work observed that BMP9 and P-JNK in the combination group rabbits were much higher than those in the PRF group, BMSC group, and Ctrl group ($P<0.05$). This indicated that PRF + BMSCs complex could more effectively induce JNK protein expression and activate the JNK pathway.

Conclusion

In this work, 28 healthy male New Zealand white rabbits purchased from the Animal Center of the University were selected to prepare BMSCs and PRFS. According to different treatment methods, all white rabbits were divided into a combination group, a PRF group, a BMSC group, and a Ctrl group, with 7 rabbits in each. The Notch1, Wnt3a, BMP9, and p-JNK proteins in four groups of rabbits were compared. The results suggested that PRF + BMSCs complex could more effectively induce the expression of Notch1 and Wnt3a, and activate the Notch1/Wnt3a signaling pathway, thus promoting the osteogenesis of ABD region and improving the repair effect. However, this work only conducted experiments on white rabbits with a small sample size, and no data collection was conducted on multiple signal pathways designed during the repair process. Therefore, animal samples will be included again later for a more comprehensive study on the mechanism of PRF + BMSCs complex in ABD treatment. In conclusion, this work gave a reference for the repair treatment of ABD.

References

1. Reis AH. From assessing risk factors to understanding, preventing, and treating cardiovascular diseases: an urgent journey. Discov Med 2022; 34(173): 199-204.

2. Tetè G, D'Orto B, Nagni M, Agostinacchio M, Polizzi E, Agliardi E. Role of induced pluripotent stem cells (IPSCS) in bone tissue regeneration in dentistry: a narrative review. J Biol Regul Homeost Agents 2020; 34(6 Suppl. 3): 1-10.

3. Cao JY, Qiu XB, Cai LL, Wu LL, Dai HT. The mechanism of notch1 signaling pathway involved in orthodontic alveolar bone remodeling in rats. Acta Med Mediterr, 2022,38(3):1941. https://doi.org/10.19193/0393-6384_2022_3_298

4. Javed Z, Khan K, Raza Q, Sadia H, Shah FA, Ahmad T, Bentivegna A, Bazzoni R, Setzer WN, Alshehri MM, Sharifi-Rad J, Daştan SD. Notch signaling and microRNA: the dynamic duo steering between neurogenesis and glioblastomas. Cell Mol Biol (Noisy-le-grand) 2021; 67(2): 33-43. https://doi.org/10.14715/cmb/2021.67.2.6

5. Slagter KW, Meijer HJA, Hentenaar DFM, Vissink A, Raghoebar GM. Immediate single-tooth implant placement with simultaneous bone augmentation versus delayed implant placement after alveolar ridge preservation in bony defect sites in the esthetic region: a 5-year randomized controlled trial. J Periodontol 2021; 92(12): 1738-1748. https://doi.org/10.1002/JPER.20-0845

6. Lu J, Wang Z, Zhang H, Xu W, Zhang C, Yang Y, Zheng X, Xu J. Bone Graft Materials for Alveolar Bone Defects in Orthodontic Tooth Movement. Tissue Eng Part B Rev 2022; 28(1): 35-51. https://doi.org/10.1089/ten.TEB.2020.0212

7. Fan Y, Cui C, Rosen CJ, Sato T, Xu R, Li P, Wei X, Bi R, Yuan Q, Zhou C. Klotho in Osx⁺-mesenchymal progenitors exerts pro-osteogenic and anti-inflammatory effects during mandibular alveolar bone formation and repair. Signal Transduct Target Ther 2022; 7(1): 155. https://doi.org/10.1038/s41392-022-00957-5

8. Hollý D, Klein M, Mazreku M, Zamborský R, Polák Š, Danišovič Ľ, Csöbönyeiová M. Stem cells and their derivatives-implications for alveolar bone regeneration: a comprehensive review. Int J Mol Sci 2021; 22(21): 11746. https://doi.org/10.3390/ijms222111746

9. van Oirschot BAJA, Geven EJW, Mikos AG, van den Beucken JJJP, Jansen JA. A Mini-Pig mandibular defect model for evaluation of craniomaxillofacial bone regeneration. Tissue Eng Part

C Methods 2022; 28(5): 193-201. https://doi.org/10.1089/ten.TEC.2022.0012

10. Huojia M, Wu Z, Zhang X, Maimaitiyiming M, Rong M. Effect of dental pulp stem cells (DPSCs) in repairing rabbit alveolar bone defect. Clin Lab 2015; 61(11): 1703-1708. https://doi.org/10.7754/clin.lab.2015.150326

11. Sperl A, Gaalaas L, Beyer J, Grünheid T. Buccal alveolar bone changes following rapid maxillary expansion and fixed appliance therapy. Angle Orthod. 2021; 91(2): 171-177. https://doi.org/10.2319/060220-504.1

12. Alici-Garipcan A, Korkusuz P, Bilgic E, Askin K, Aydin HM, Ozturk E, Inci I, Ozkizilcik A, Kamile Ozturk K, Piskin E, Vargel I. Critical-size alveolar defect treatment via TGF-ß3 and BMP-2 releasing hybrid constructs. J Biomater Sci Polym Ed 2019; 30(5): 415-436. https://doi.org/10.1080/09205063.2019.1571397

13. Rawashdeh MA, Telfah H. Secondary alveolar bone grafting: the dilemma of donor site selection and morbidity. Br J Oral Maxillofac Surg 2008; 46(8): 665-670. https://doi.org/10.1016/j.bjoms.2008.07.184

14. Linderup BW, Küseler A, Jensen J, Cattaneo PM. A novel semiautomatic technique for volumetric assessment of the alveolar bone defect using cone beam computed tomography. Cleft Palate Craniofac J 2015; 52(3): e47-55. https://doi.org/10.1597/13-287

15. Martinelli F, Diaz AB, Afonso RH, Araújo MTS. Collagen membrane and distraction osteogenesis for correcting alveolar bone defects: an animal pilot study. J World Fed Orthod 2022; 11(4): 130-135. https://doi.org/10.1016/j.ejwf.2022.05.003

16. Dominiak M, Dominiak S, Targonska S, Gedrange T. Three-dimensional bone block planning for mandibular sagittal bone defect reconstruction. J Healthc Eng 2020; 2020: 8829288. https://doi.org/10.1155/2020/8829288

17. Yamauchi K, Nogami S, Kataoka Y, Koyama S, Lethaus B, Takahashi T. Cortical bone repositioning technique for horizontal alveolar bone augmentation: a case series. Int J Periodontics Restorative Dent 2018; 38(5): 691-697. https://doi.org/10.11607/prd.2839

18. Wehner C, Bertl K, Durstberger G, Arnhart C, Rausch-Fan X, Stavropoulos A. Characteristics and frequency distribution of bone defect configurations in peri-implantitis lesions-A series of 193 cases. Clin Implant Dent Relat Res 2021; 23(2): 178-188. https://doi.org/10.1111/cid.12961

19. Kim SH, Kim KH, Seo BM, Koo KT, Kim TI, Seol YJ, Ku Y, Rhyu IC, Chung CP, Lee YM. Alveolar bone regeneration by transplantation of periodontal ligament stem cells and bone marrow stem cells in a canine peri-implant defect model: a pilot study. J Periodontol 2009; 80(11): 1815-1823. https://doi.org/10.1902/jop.2009.090249

20. Kawata T, Kohno S, Fujita T, Sugiyama H, Tokimasa C, Kaku M, Tanne K. New biomaterials and methods for craniofacial bone defect: chondroid bone grafts in maxillary alveolar clefts. J Craniofac Genet Dev Biol 2000; 20(1): 49-52.

21. Yu K, Liu W, Su N, Chen H, Wang H, Tan Z. Evaluation of resorption and osseointegration of autogenous bone ring grafting in vertical bone defect with simultaneous implant placement in dogs. J Oral Implantol 2021; 47(4): 295-302. https://doi.org/10.1563/aaid-joi-D-19-00199

22. Wang H, Sun XC, Zhang D, Li JH, Yin LQ, Yan YF, Ma X, Xia HF. Active bone material containing modified recombinant human bone morphogenetic protein 2 induces bone regeneration in the alveolar process cleft in rabbits. Artif Organs 2021; 45(7): O207-O222. https://doi.org/10.1111/aor.13889

23. Nadal E, Sabás M, Dogliotti P, Espósito R. Secondary alveolar bone grafting: our experience with olecranon bone graft. J Craniofac Surg 2010; 21(2): 371-374. https://doi.org/10.1097/SCS.0b013e3181cf6084

24. Ren S, Zhao H, Pan Y. [Evaluation of the degree and pattern of alveolar bone defect inaggressive periodontitis using cone-beam CT]. Zhonghua Kou Qiang Yi Xue Za Zhi 2015; 50(5): 291-296.

25. Saulacic N, Martín MS, Vila PG, García AG. Bone defect formation during implant placement following alveolar distraction. Int J Oral Maxillofac Implants 2007; 22(1): 47-52.

26. Nguyen PD, Lin CD, Allori AC, Ricci JL, Saadeh PB, Warren SM. Establishment of a critical-sized alveolar defect in the rat: a model for human gingivoperiosteoplasty. Plast Reconstr Surg 2009; 123(3): 817-825. https://doi.org/10.1097/PRS.0b013e31819ba2f4

27. Madi M, Zakaria O, Kasugai S. Coated vs uncoated implants: bone defect configurations after progressive peri-implantitis in dogs. J Oral Implantol 2014; 40(6): 661-669. https://doi.org/10.1563/AAID-JOI-D-12-00089

28. Yang LS, Yan JW, Zheng H, Ni R, Han XK, Chang X. [Comparative study of processed autogenous tooth bone and xenogeneic bovine bone in repairing an alveolar bone defect]. Hua Xi Kou Qiang Yi Xue Za Zhi 2018; 36(4): 372-377. Chinese. https://doi.org/10.7518/hxkq.2018.04.005